

1
2
3
4
5
6
7
8
9
10
11
12
13
14
15
16
17
18
19
20
21
22
23
24
25
26
27
28

Determination of acid dissociation constants of flavin analogues by capillary zone electrophoresis

Yuki Tanikami,¹ Takuma Tagami,¹ Mayu Sakamoto,² Yukihiro Arakawa (0000-0003-1000-5799),^{3*} Hitoshi Mizuguchi (0000-0003-2396-6812),³ Yasushi Imada (0000-0002-4844-5418),³ and Toshio Takayanagi (0000-0002-5767-1126)^{3*}

¹ Graduate School of Advanced Technology and Science, Tokushima University, 2-1 Minamijyousanjima-cho, Tokushima 770-8506, Japan

² Department of Chemical Science and Technology, Faculty of Engineering, Tokushima University, 2-1 Minamijyousanjima-cho, Tokushima 770-8506, Japan

³ Graduate School of Technology, Industrial and Social Sciences, Tokushima University, 2-1 Minamijyousanjima-cho, Tokushima 770-8506, Japan

*Correspondence should be addressed to the following authors:

Toshio Takayanagi (Prof.) and Yukihiro Arakawa (Assist. Prof.)

Graduate School of Technology, Industrial and Social Sciences

Tokushima University

2-1 Minamijyousanjima-cho, Tokushima 770-8506, Japan

toshio.takayanagi@tokushima-u.ac.jp (T. T.); arakawa.yukihiro@tokushima-u.ac.jp (Y. A.)

Keywords: Acid dissociation constant / Flavin analogues / Instable substances / Capillary zone electrophoresis

Abbreviations: FL, flavin; RF, riboflavin; LC, lumichrome

29 **Abstract**

30 Acid dissociation constants (pK_a) of 9 kinds of flavin analogues as molecular catalyst
31 candidates were determined by CZE. Although some of the analogues are instable
32 and degradable under the light-exposure or in alkaline aqueous solutions, the effective
33 electrophoretic mobility of the flavin analogue of interest has been measured with the
34 residual substance. The pK_a values of the flavin analogues were analyzed through the
35 changes in the effective electrophoretic mobility with varying pH of the separation
36 buffer. One or two steps pK_a values were determined by the analysis. One of the
37 degraded species from the flavin analogues, lumichrome, was also detected in the
38 CZE analysis, and its pK_a values were also determined. While coexisting impurities
39 generated over the storage conditions were found in some analogues, the pK_a values
40 of the target analogues were successfully determined with the help of the CZE
41 separations. A pressure-assisted CZE was utilized for the determination or the
42 estimation of the pK_a values of such analogues as possessing carboxylic acid moiety.

43 **1 Introduction**

44 Redox reactions are essential on organic syntheses, and molecular catalysts inducing
45 redox reactions are intensively investigated. For example, flavin analogues contain
46 heterocyclic isoalloxazine (flavin, FL) ring and they are one of the famous redox-active
47 molecular catalysts [1]. In nature, the heterocyclic isoalloxazine rings are utilized as
48 an active center of the redox enzymes, in which xenobiotic substrates are metabolized
49 through the oxidations such as dehydrogenation and monooxygenation. Thus, FL
50 analogues are expected to work as oxidative molecular catalysts without any active
51 center of metal ion [2-4]. On the activity design of the molecular catalysts, acid
52 dissociation constant (pK_a) is one of the key parameters. Since pK_a values and redox
53 potentials are closely related to each other, experimentally determining the pK_a values
54 of the FL analogues would be highly valuable on developing their redox catalysis.
55 However, some of the FL analogues are not stable against light or alkaline base [5,6],
56 which hampers the conventional methods for the pK_a determination.

57 Acid dissociation constants have classically been determined by potentiometric and
58 spectrophotometric titrations. However, the homogeneous titrations are not applicable
59 to such substances as are not pure or degradable. Spectrum shift is indispensable for

60 the pK_a determination by the spectrophotometric titration. On the contrary, CZE
61 determination of acid dissociation constants is based on the changes in the effective
62 electrophoretic mobility with protonation/deprotonation reaction under varying pH [7],
63 and the CZE analysis is applicable to such substances as containing impurities or
64 degradable under the measurement conditions [8-11]. Acid dissociation constants of
65 alkaline-degradable phenolphthalein [8], labile drug compounds [9], acid-degradable
66 tetrabromophenolphthalein ethyl ester [10], and heat-degradable bupropion [11] have
67 been determined by utilizing the prominent characteristics of the CZE analysis.

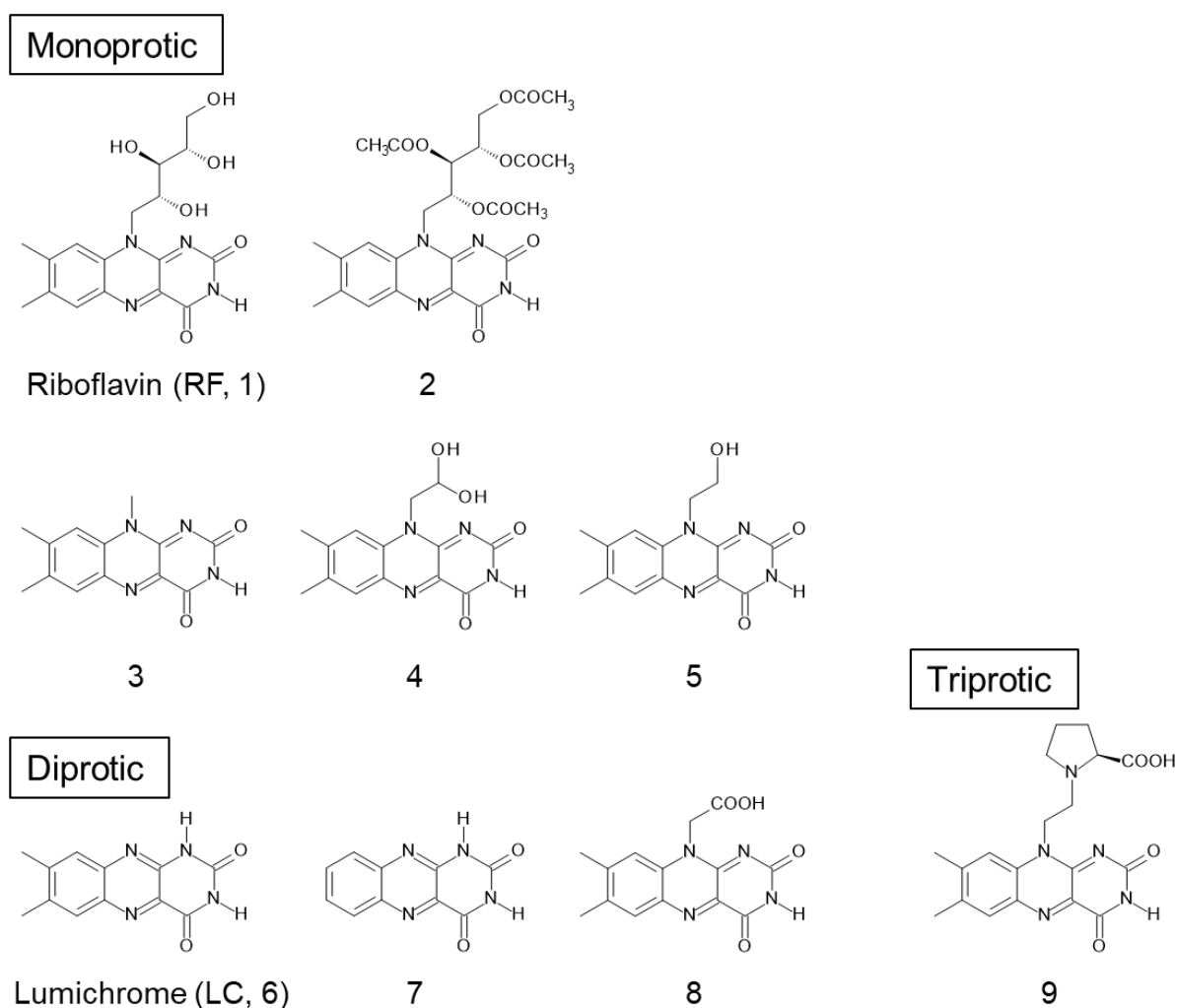
68 In this study, acid dissociation constants of 9 kinds of FL analogues were determined
69 by CZE through the measurements of their effective electrophoretic mobility. Although
70 some of the FL analogues were degradable under alkaline conditions and/or light
71 exposure, the acid dissociation constants were successfully determined by CZE. Aim
72 of this study is determining the pK_a values of such difficult substances, even though
73 they are conditional values. The target analogue was resolved from the degraded
74 species, and changes in the effective electrophoretic mobility of the analogue gave the
75 pK_a value(s). Some analogues contained unavoidable impurities formed under the
76 storage conditions, the impurities were also resolved by CZE and the pK_a value(s) of
77 the target analyte was also determined. Acid dissociation constants of the degraded
78 species, as well as those of the impurities, were determined through the mobility
79 change.

80 **2 Materials and methods**

81 **2.1 Chemicals**

82 Riboflavin and lumichrome, as well as all other reagents used for the synthesis of its
83 analogues, were purchased from commercial supplies and used without further
84 purification, besides *N*,3,4-trimethylaniline that was prepared according to the
85 literature procedure [12]. Flavin analogues prepared and examined in this study are
86 shown in Figure 1. They are categorized as monoprotic (5 analogues), diprotic (3
87 analogues), and triprotic (1 analogue) acids. The analogues were synthesized
88 according to the literature previously reported, and the details are written in Supporting
89 Information. Separation buffers of the CZE were prepared with following buffer
90 components: 0.010 mol L⁻¹ H₃PO₄ – NaOH (pH 2.38 – 3.21); 0.010 mol L⁻¹ HCOOH

91 – NaOH (pH 3.13 – 3.53); 0.010 mol L⁻¹ CH₃COOH – NaOH (pH 4.08 – 4.75); 0.010
 92 mol L⁻¹ MES – NaOH (pH 5.48 – 6.42); 0.010 mol L⁻¹ HEPES – NaOH (pH 6.78 –
 93 8.00); 0.010 mol L⁻¹ TAPS – NaOH (pH 8.02 – 9.28); 0.010 mol L⁻¹ CHES – NaOH
 94 (pH 8.77 – 10.36); 0.010 mol L⁻¹ CAPS – NaOH (pH 9.88 – 11.27). NaOH was also
 95 used in the alkaline pH conditions (pH 11.48 – 12.38). Ionic strength of the separation
 96 buffers was adjusted at 0.010 mol L⁻¹ by adding adequate amount of NaCl. Internal
 97 standards of naphthalene-1-sulfonate (1-NS⁻, sodium salt) and *N*-ethylquinolinium
 98 (EtQ⁺, iodate salt) were from Tokyo Chemical Industry (Tokyo, Japan). Other reagents
 99 were of analytical grade. Water used was purified by Milli-Q Gradient A10 (Merck-
 100 Millipore, Milford, MA, USA).



101

102 **Figure 1.** Structures of flavin analogues examined in this study.

103

104 **2.2 Apparatus**

105 An Agilent Technologies (Waldbronn, Germany) ³DCE was used for the CZE
106 measurements equipped with a photodiode array detector. A fused silica capillary (GL
107 Sciences, Tokyo, Japan) was set in a cassette cartridge, and the cartridge was
108 installed in the CZE system. Dimensions of the capillary were 64.5 cm in total length,
109 56 cm in the effective length from the sample injection point to the detection point, 50
110 μm in inner diameter and 375 μm in outer diameter. A short capillary was also used in
111 the pressure-assisted CZE at the acidic pH conditions; the total length and the
112 effective length of the capillary were 48.5 cm and 40 cm, respectively.

113 A Waters (Milford, MA, USA) ACQUITY UPLC with LCT Premire XE was used as an
114 LC-MS system; a reversed phase column of BEH C18 (Waters, 50 mm \times 2.1 mm i.d.,
115 1.7 μm) was attached to the LC-MS system. Flow rate of the eluent was set at 1 mL
116 min^{-1} , the MS polarity was ESI (+), and the injection volume was 20 μL . JASCO (Tokyo,
117 Japan) PU-2080 plus and UV-2075 plus were used as a conventional RP-HPLC
118 system with UV detection. An RP column of Unison UK-C18 (75 mm length \times 4.6 mm
119 i.d., 3 μm particle size; Imtakt, Kyoto, Japan) was attached to the system. An eluent of
120 70/30 (v/v) water/ethanol was used. NMR spectra were recorded using JEOL (Tokyo,
121 Japan) JNM-ECZ-400S (¹H, 400 MHz). Chemical shifts are reported in ppm using TMS
122 or the residual solvent peak as a reference. An HM-25G pH meter (TOA DKK, Tokyo,
123 Japan) was used for the pH measurements of the separation buffers, after being
124 calibrated daily with standard pH solutions. UV-LED light was used to expose and to
125 degrade the FL analogues by NS375LIM (Emission maximum at 375 \pm 5 nm, 1.4 W;
126 Nitride Semiconductors, Naruto, Japan).

127

128 **2.3 Procedure**

129 Stock solutions of FL analogues were prepared as ethanol solution at mmol L^{-1} level.
130 The stock solution was diluted with water, and a solution of an FL analogue was
131 prepared at the concentration of about $5 \times 10^{-5} \text{ mol L}^{-1}$; it was used as a sample
132 solution for the CZE measurements. Monoanionic 1-NS⁻ or monocationic EtQ⁺ was
133 added in the sample solution as an internal standard of the electrophoretic mobility.
134 Ethanol at the concentration of 3 %(v/v) was also contained in the sample solution to
135 monitor the electroosmotic flow (EOF). After the separation capillary being equilibrated

136 with a separation buffer, the sample solution was introduced into the capillary from the
 137 anodic end by applying a pressure of 50 mbar for 5 s. Both ends of the capillary were
 138 dipped in the separation buffer vials, and a DC voltage of 25 kV was applied for the
 139 CZE. During the CZE, the capillary was thermostat at 25 °C by circulating a constant-
 140 temperature air in the cassette cartridge. An analyte of the FL analogue and the
 141 internal standard were photometrically detected at 220 nm. Effective electrophoretic
 142 mobility, μ_{eff} , was calculated with the migration times of the analyte and the EOF in an
 143 ordinary manner. Acid dissociation constants of FL analogues were analyzed through
 144 the change in μ_{eff} , after standardized with the cationic or anionic internal standard.
 145 On the measurements of the effective electrophoretic mobility at weakly acidic pH
 146 conditions over 2.38 – 4.75, the velocity of electroosmotic flow was not fast enough,
 147 and pressure-assisted CZE [13,14] was made. A constant pressure of 30 mbar was
 148 applied to the inlet vial of the separation buffer during the electrophoresis.

149

150 **2.4 Determination of acid dissociation constants of FL analogues** 151 **by CZE**

152 Three types of the acid dissociation equilibria are included in the FL analogues of
 153 monoprotic, diprotic, and triprotic acids. For monoprotic FL analogues, HA, the charge
 154 changes from 0 to -1 by the one-step acid dissociation reaction of the imide moiety.
 155 The equilibrium reaction and its acid dissociation constant are written as in Eqs. (1)
 156 and (2), respectively. Fractions of the species are related with the effective
 157 electrophoretic mobility of the analogue, μ_{eff} , and the μ_{eff} value at a particular pH
 158 condition is given in Eq. (3).



$$160 K_a = \frac{[\text{H}^+][\text{A}^-]}{[\text{HA}]} \quad (2)$$

$$161 \mu_{\text{eff}} = \frac{[\text{A}^-] \times \mu_{\text{ep,A}}}{[\text{HA}] + [\text{A}^-]} = \frac{10^{-\text{p}K_a} \times \mu_{\text{ep,A}}}{10^{-\text{pH}} + 10^{-\text{p}K_a}} \quad (3)$$

162 In Eq. (2), $[\text{H}^+]$ is conventionally used instead of a_{H^+} , and K_a written in Eq. (2) is exactly
 163 a mixed equilibrium constant. Value of $\mu_{\text{ep,A}}$ is the electrophoretic mobility of the
 164 monoanionic FL species. The protonated FL species, HA, is neutral, and its
 165 electrophoretic mobility can be set as zero; Eq. (3) is thus given. A series of the pairs
 166 of pH and μ_{eff} value were put in Eq. (3), and the values of $\mu_{\text{ep,A}}$ and $\text{p}K_a$ were optimized

167 by a non-linear least-squares analysis [8,10]. Since the measured electrophoretic
 168 mobility may deviate under the variation of experimental conditions, the value of μ_{eff}
 169 was standardized with the electrophoretic mobility of 1-NS⁻, $\mu_{\text{eff},1\text{-NS}}$, and the
 170 standardized value of $\mu_{\text{eff}} / \mu_{\text{eff},1\text{-NS}}$ was used for the analysis. Because 1-NS⁻ is a
 171 monoanion over the wide pH range and its electrophoretic mobility is essentially
 172 identical under the experimental conditions, and it was chosen as an internal standard.
 173 On analyzing the $\text{p}K_{\text{a}}$ value, a software of R program (Ver. 3.6.2) was used on the
 174 basis of nonlinear least-squares regression [15]. Higher ionic strength would bias the
 175 $\text{p}K_{\text{a}}$ value from its thermodynamic one, $\text{p}K_{\text{a}}^{\circ}$. However, the $\text{p}K_{\text{a}}$ variation is generally
 176 ~ 0.1 for monoprotic acid at ionic strength of 0.10 mol L⁻¹. The $\text{p}K_{\text{a}}$ values are
 177 determined at ionic strength of 0.010 mol L⁻¹, and the values determined in this study
 178 would differ little from the thermodynamic ones; less than 0.1.

179 For diprotic FL analogues, H₂A, the charge changes from 0 to -2 by the two-steps acid
 180 dissociation reactions as in Eq. (4). The stepwise acid dissociation constants, $K_{\text{a}1}$ and
 181 $K_{\text{a}2}$, are written in Eq. (5). The effective electrophoretic mobility of an FL analogue at
 182 a particular pH condition is given in Eq. (6).



$$184 \quad K_{\text{a}1} = \frac{[\text{H}^+][\text{HA}^-]}{[\text{H}_2\text{A}]}, \quad K_{\text{a}2} = \frac{[\text{H}^+][\text{A}^{2-}]}{[\text{HA}^-]} \quad (5)$$

$$185 \quad \mu_{\text{eff}} = \frac{[\text{HA}^-] \times \mu_{\text{ep,HA}} + [\text{A}^{2-}] \times 2\mu_{\text{ep,HA}}}{[\text{H}_2\text{A}] + [\text{HA}^-] + [\text{A}^{2-}]} = \frac{10^{-\text{pH}-\text{p}K_{\text{a}1}} \times \mu_{\text{ep,HA}} + 10^{-\text{p}K_{\text{a}1}-\text{p}K_{\text{a}2}} \times 2\mu_{\text{ep,HA}}}{10^{-2\text{pH}} + 10^{-\text{pH}-\text{p}K_{\text{a}1}} + 10^{-\text{p}K_{\text{a}1}-\text{p}K_{\text{a}2}}} \quad (6)$$

186 Value of $\mu_{\text{ep,HA}}$ is the electrophoretic mobility of the monoanionic FL species. The
 187 electrophoretic mobility of dianionic FL species is assumed to be twice to the
 188 monoanionic FL species [8,16]. A series of the pairs of pH and μ_{eff} were put in Eq. (6),
 189 and the values of $\text{p}K_{\text{a}1}$ and $\text{p}K_{\text{a}2}$, as well as $\mu_{\text{ep,HA}}$, were optimized by a non-linear
 190 least-squares analysis in a similar manner to the analysis of the one-step $\text{p}K_{\text{a}}$ [16].

191 3 Results and discussion

192 3.1 Determination of an acid dissociation constant of RF

193 Prior to the determination of the synthesized FL analogues, an acid dissociation
 194 constant of RF was determined through the changes in the effective electrophoretic
 195 mobility in CZE. Riboflavin is a monoprotic acid, and its charge changes from 0 to -1

196 by the acid dissociation reaction of the imide moiety. Electropherograms of RF at
 197 several pH conditions are shown in Fig. S1 A. The migration time of RF got longer with
 198 the increase in pH, suggesting that RF is more anionic at alkaline pH conditions.
 199 Changes in the standardized electrophoretic mobility of RF are shown in Fig. S1 B.
 200 Analysis of the results with Eq. (3) gave a pK_a value of 10.29 ± 0.06 (mean \pm standard
 201 error) by a least-squares analysis. The result agrees with the reported pK_a value of
 202 10.2 [17]. The pK_a values are summarized in Table 1.

203

204 **Table 1.** Acid dissociation constants of RF and its photo-degradant of LC

	pK_{a1} (this study) ^{a)}	pK_{a2} (this study) ^{a)}	pK_{a1} (ref.)	pK_{a2} (ref.)
RF, 1	10.29 ± 0.06 10.24 ± 0.03 ^{b)}	N/A ^{c)}	10.2 ^{d)} 10.64 ^{e)}	N/A
LC, 6	8.36 ± 0.02 (degradant)	(13.54 ± 0.10) ^{f)}	8.2 ^{g)}	11.4 ^{g)}

205 ^{a)} Error: standard error.

206 ^{b)} Determined under the degraded conditions.

207 ^{c)} Not applicable.

208 ^{d)} Ref. 17.

209 ^{e)} Ref. 19. Determined by spectrophotometric titration.

210 ^{f)} Estimated value by extrapolation.

211 ^{g)} Ref. 18.

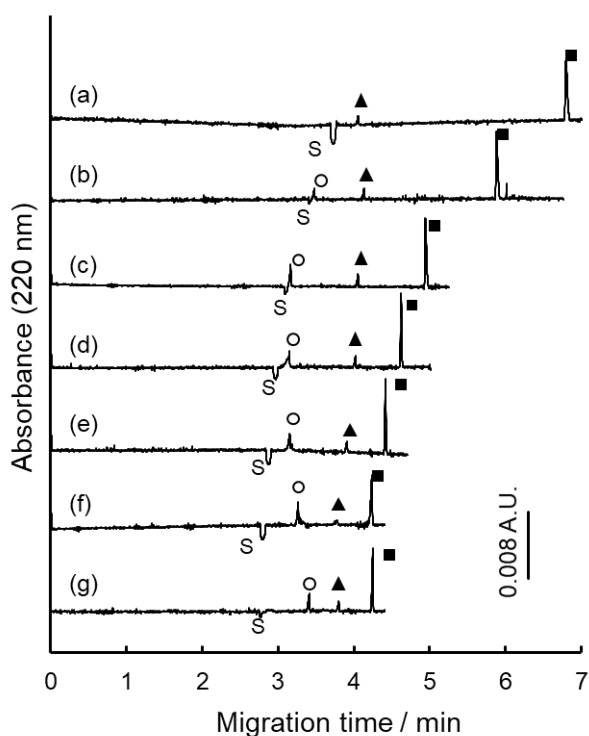
212

213 It is known that RF is degradable by light-exposure to form LC [5]. When the UV light
 214 was irradiated to an aliquot of 3 mL RF solution containing 1.0×10^{-4} mol L⁻¹ RF, a CZE
 215 determination of RF suggested that the residual RF gradually decreased with the
 216 irradiation time and that the residual concentration of RF was about 60 % by the 120
 217 min irradiation. Another distinct peak-signal was detected in the electropherograms
 218 with the irradiated solution, and the signal intensity complementary increased along
 219 with the decrease in the RF concentration. Therefore, the peak signal would be
 220 attributed to a degraded substance. The photo-degraded solution was analyzed by a
 221 conventional RP-HPLC and the LC-MS. The retention time of a degradant was about
 222 20 min in the RP-HPLC, while that of RF was about 5 min. A mass number of 243.09
 223 was detected by LC-MS with the substance of the longer retention time; it is attributed
 224 to protonated LC.

225 The acid dissociation constant of RF was also determined under the degraded
 226 conditions. An aliquot of aqueous RF solution at the concentration of 5×10^{-4} mol L⁻¹
 227 was exposed under a UV lamp for 120 min, and the solution was diluted by 10 times

228 and used for the pK_a determination after adding $2 \times 10^{-5} \text{ mol L}^{-1}$ 1-NS⁻ as an internal
 229 standard and 3 %(v/v) ethanol as an EOF marker. Electropherograms of the degraded
 230 RF are shown in Figure 2; the residual RF (open circle) is still detected with the
 231 degraded solution. It can be noticed that additional peak indicated with the filled
 232 triangle is also detected in the electropherograms, as mentioned above. The migration
 233 time of RF, as well as that of the degradant, got longer with increasing pH of the
 234 separation buffer; both RF and the degradant become more anionic.

235



236

237 **Figure 2.** Electropherograms of RF at several
 238 pH conditions after UV-light exposure for 120
 239 min. pH conditions: (a), 7.82; (b), 8.45; (c),
 240 9.05; (d), 9.70; (e), 10.12; (f), 10.77; and (g),
 241 11.48. Symbols: ○, RF; ▲, LC as a degradant
 242 from RF; ■, 1-NS; S, solvent (EOF). Sample
 243 solution: $5 \times 10^{-5} \text{ mol L}^{-1}$ RF (partly degraded) +
 244 $2 \times 10^{-5} \text{ mol L}^{-1}$ 1-NS⁻ (I.S.) + 3 %(v/v) ethanol.
 245 Separation buffers are written in the text. CZE
 246 conditions: applied voltage, 25 kV; sample
 247 injection, 50 mbar \times 5 s; detection wavelength,
 248 220 nm; capillary temperature, 25 °C.

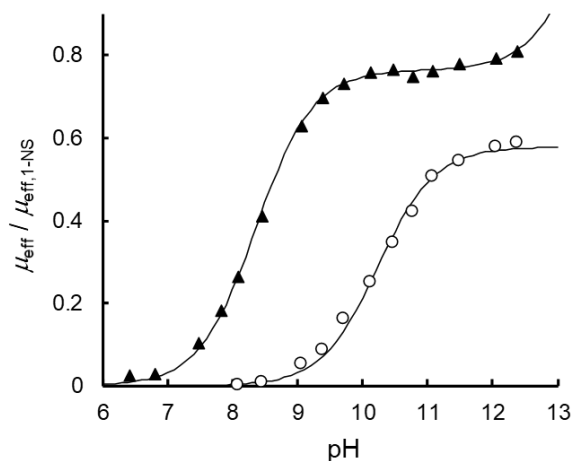
249

250 Changes in the effective electrophoretic mobility, μ_{eff} , are shown in Figure 3 after
 251 standardized with $\mu_{\text{eff},1\text{-NS}}$. The standardized μ_{eff} of the monoanionic degradant at pH
 252 around 11 is larger than RF, and the degradant would possess lighter molecular mass

253 than RF. While RF showed monoprotic profile of the mobility change, the μ_{eff} of the
254 degradant tended to increase at the alkaline pH conditions over 12. The acid
255 dissociation constant of RF under the degraded conditions was also determined with
256 Eq. (3), and pK_a value of 10.24 ± 0.03 was obtained (Table 1). The pK_a value agreed
257 with the freshly prepared RF solution, as well as the reference value [17]. Therefore,
258 usefulness of the CZE analysis, electrophoretic separation of the target analyte from
259 coexisting substances [8-11], was also demonstrated in this study.

260 Acid dissociation constants of the degradant were also determined through the
261 changes in the effective electrophoretic mobility. The increased μ_{eff} value at the
262 alkaline pH conditions suggested the formation of a dianionic species. The CZE
263 measurements, however, are limited under the pH conditions below ~ 12 , because the
264 higher pH conditions accompany the high salt concentrations, yielding much Joule's
265 heat and temperature increase. Since the dianionic species is twice in its charge from
266 the monoanionic species and its molecular mass is almost identical to the monoanionic
267 species, μ_{eff} value of the dianionic species is supposed to be twice to the monoanionic
268 species. This assumption was valid in phenolphthalein [8] and fluorescein derivatives
269 [16]. Equation (6) was thus used for the determination of the two steps of the pK_a
270 values; $pK_{a1} = 8.36 \pm 0.02$ and $pK_{a2} = 13.54 \pm 0.10$ were obtained by the least-squares
271 analysis. It should be taken care of that the pK_{a2} value obtained in this study is the
272 results of the extrapolated analysis. The pK_{a1} value obtained in this study agreed well
273 with the reported value of LC ($pK_{a1} = 8.2$) [18], and the degradant detected in this study
274 would be LC. Lumichrome is diprotic acid with the imide moiety and N(1)-H [18], and
275 two steps of the mobility change would also suggest the degradant to be LC. Therefore,
276 another usefulness of the CZE analysis is also demonstrated in this study; the
277 degradant can directly be analyzed without any isolation from the reaction mixture. On
278 the other hand, the pK_{a2} value obtained in this study did not agree with the reported
279 value of 11.4 [18]. The μ_{eff} value of the degradant LC slightly changed at the pH
280 conditions at around 11, suggesting the lack of the acid dissociation equilibrium at this
281 pH range; the reference value determined by a spectrophotometric titration would not
282 be correct.

283



284

285 **Figure 3.** Changes in the effective
 286 electrophoretic mobility of RF and LC as a
 287 degradant from RF. The electrophoretic
 288 mobility was standardized with 1-NS⁻ as an
 289 internal standard. Symbols: \circ , RF; \blacktriangle , LC as a
 290 degradant. The curves are drawn with the
 291 optimized results. The CZE conditions are the
 292 same as in Fig. 2.

293

294 **3.2 Determination of acid dissociation constants of FL analogues** 295 **by CZE**

296 **3.2.1 Acid dissociation constant of FL analogue 2**

297 Riboflavin tetraacetate (FL analogue 2) is a monoprotic acid, and its charge changes
 298 from 0 to -1 by the acid dissociation reaction of the imide moiety. Electropherograms
 299 at several pH conditions are shown in Figure S2 A, and the changes in μ_{eff} are shown
 300 in Figure S2 B after standardized with $\mu_{\text{eff},1\text{-NS}}$. Analysis of the changes in μ_{eff} with Eq.
 301 (3) gave a $\text{p}K_{\text{a}}$ value of 10.21 ± 0.05 .

302 An adjacent peak was detected just after the FL analogue 2. A small portion of FL
 303 analogue 2 would have hydrolyzed in the alkaline separation buffer during the CZE.
 304 When FL analogue 2 at its concentration of $1.0 \times 10^{-4} \text{ mol L}^{-1}$ was treated in an alkaline
 305 solution of $5 \times 10^{-4} \text{ mol L}^{-1}$ NaOH for 50 min, additional peak signal was detected by
 306 CZE as an adjacent peak behind to the peak signal of FL analogue 2. Thus, the newly
 307 detected signal would be attributed to the hydrolyzed species of FL analogue 2; one
 308 or more ester moieties are hydrolyzed to form alcohol group(s). Even under the
 309 alkaline-degraded conditions, the acid dissociation constant of FL analogue 2 was

310 successfully determined as $pK_a = 10.24 \pm 0.04$. The pK_a value is close to the one
311 determined with the freshly prepared solution.

312 The alkaline-treated FL analogue 2 solution was analyzed by RP-HPLC and LC-MS.
313 A certain number (~10) of peaks were detected by a conventional RP-HPLC-UV
314 detected at 220 nm. The LC-MS chromatograms are shown in Figure S3. The mass
315 numbers detected by the LC-MS were 545.188 (FL analogue 2 +H), 503.178, 419.157,
316 and 377.146. The Each mass number corresponds to deacetylated substances from
317 FL analogue 2, and the mass number 377.146 is equivalent to RF. Therefore, the
318 newly detected peaks in Figure S2 would be attributed to the hydrolyzed substances
319 from FL analogue 2.

320

321 **3.2.2 Acid dissociation constant of FL analogue 3**

322 Lumiflavin (FL analogue 3) is also a monoprotic acid, and its charge similarly changes
323 from 0 to -1 by the acid dissociation reaction of the imide moiety. Electropherograms
324 are shown in Figure S4 A, and the changes in μ_{eff} are shown in Figure S4 B after
325 standardized with $\mu_{\text{eff},1-\text{NS}}$. An additional peak signal indicated with filled triangle was
326 detected with FL analogue 3; it would be attributed to an impurity formed under the
327 storage conditions. An additional peak was also detected with the FL analogue 3
328 solution by a conventional RP-HPLC-UV detection; LC-MS analysis gave a substance
329 of mass number of 243.09. The mass number is equivalent to LC, and the impurity
330 would be LC. The migration time of FL analogue 3, as well as the additional peak
331 signal, got longer than the EOF with the increase in pH as in the case of RF. Analysis
332 of the changes in μ_{eff} of FL analogue 3 with Eq. (3) gave a pK_a value of 10.38 ± 0.04 .
333 Unfortunately, the additional peak was not detected in the alkaline separation buffer,
334 it would have been overlapped with FL analogue 3. The monoprotic behavior of the
335 additional peak was analyzed with Eq. (3), and a pK_a value of 8.29 ± 0.02 was obtained;
336 the pK_a value is close to that of LC. The usefulness of the CZE analysis is also
337 demonstrated with such substance as containing impurity, as well as the pK_a analysis
338 of the impurity.

339

340 **3.2.3 Acid dissociation constant of FL analogue 4**

341 10-(2,2-Dihydroxyethyl)-7,8-dimethylisoalloxazine (FL analogue 4) is also a
342 monoprotic acid, and its charge changes from 0 to -1 by the acid dissociation reaction
343 of the imide moiety. Electropherograms are shown in Figure S5 A, and the changes in
344 μ_{eff} are shown in Figure S5 B after standardized with $\mu_{\text{eff},1-\text{NS}}$. A peak signal
345 corresponding to FL analogue 4 disappeared at pH 12.05 (Figure S5 A(f)). The result
346 suggests that FL analogue 4 has decomposed at the alkaline conditions. An additional
347 peak signal indicated with filled triangle was also detected with FL analogue 4 as in
348 the case of FL analogue 3. Although the migration time of the EOF became faster at
349 alkaline pH conditions, the peak signal of FL analogue 4 much delayed from the EOF
350 at alkaline pH conditions. Analysis of the changes in μ_{eff} with Eq. (3) gave a $\text{p}K_{\text{a}}$ value
351 of 10.22 ± 0.08 for FL analogue 4. An acid dissociation constant of the impurity was
352 also determined with Eq. (3), and a $\text{p}K_{\text{a}}$ value of 8.40 ± 0.02 was obtained. LC-MS
353 analysis gave a mass number of 243.09, and the impurity was also found to be LC.

354

355 **3.2.4 Acid dissociation constant of FL analogue 5**

356 10-(2-Hydroxyethyl)-7,8-dimethylisoalloxazine (FL analogue 5) is also a monoprotic
357 acid, and its charge changes from 0 to -1 by the acid dissociation reaction of the imide
358 moiety. Electropherograms are shown in Figure S6 A, and the changes in μ_{eff} are
359 shown in Figure S6 B after standardized with $\mu_{\text{eff},1-\text{NS}}$. A peak signal corresponding to
360 FL analogue 5 was detected. Although a peak signal of an impurity or the degradant
361 was detected at pH around 10.5, it did not interfere with the $\text{p}K_{\text{a}}$ analysis of FL
362 analogue 5. The additional peak signal was not detected when FL analogue 5 was
363 freshly prepared, and therefore, it would be generated under light exposure. The
364 migration time of FL analogue 5 got longer than the EOF with the increase in pH as in
365 the case of RF. Analysis of the changes in μ_{eff} with Eq. (3) gave a $\text{p}K_{\text{a}}$ value of
366 10.35 ± 0.04 for FL analogue 5.

367

368 **3.2.5 Acid dissociation constants of FL analogue 7**

369 Alloxazine (FL analogue 7) is a diprotic acid, and its charge changes from 0 to -2 by
370 the acid dissociation reactions of the imide moiety and N(1)-H. Electropherograms are
371 shown in Figure S7 A, and the changes in μ_{eff} are shown in Figure S7 B after

372 standardized with $\mu_{\text{eff},1-\text{NS}}$. The μ_{eff} value increased in the pH range from 7 to 9, and an
 373 acid dissociation equilibrium is applied in this pH range. The μ_{eff} value further
 374 increased in the pH range over 11. This increase would be attributed to the 2nd step
 375 of the deprotonation. Two steps of the acid dissociation equilibria are analyzed with
 376 Eq. (6) in a similar manner to LC, and the pK_{a} values of $pK_{\text{a}1} = 8.07 \pm 0.01$ and $pK_{\text{a}2} =$
 377 12.96 ± 0.4 were obtained by the least-squares analysis. It should also be taken care
 378 of that the $pK_{\text{a}2}$ value obtained in this study is the results of the extrapolated analysis,
 379 as in the case of LC. It can be noted that both $pK_{\text{a}1}$ and $pK_{\text{a}2}$ values of FL analogue 7
 380 are smaller than those of LC. The result would be attributed to the lack of two methyl
 381 groups of electron donating moiety.

382

383 3.2.6 Acid dissociation constants of FL analogue 8 at weakly alkaline pH region

384 7,8-Dimethyl-10-carboxymethylisalloxazine (FL analogue 8) is a diprotic acid, and its
 385 charge changes from 0 to -2 by the acid dissociation equilibria of a carboxylic acid
 386 moiety and an imide moiety. The carboxylic acid moiety would dissociate at weakly
 387 acidic pH region, and the imide moiety at weakly alkaline pH region.
 388 Electropherograms in the neutral to weakly alkaline pH range are shown in Figure S8,
 389 and the changes in μ_{eff} are shown in Figure 4 A after standardized with $\mu_{\text{eff},1-\text{NS}}$. A peak
 390 signal attributed to FL analogue 8, as well as an impurity, is detected in the
 391 electropherograms. According to the presence of the carboxylate moiety, FL analogue
 392 8 is anionic in the pH range between 7.9 and 12.0. On the other hand, detection of FL
 393 analogue 8 was difficult at acidic pH conditions below 4.5, because the electroosmotic
 394 flow was too slow at the acidic pH conditions to detect the anionic species. In Figure
 395 4 A, the μ_{eff} value of FL analogue 8 increased in the pH range at around 11, suggesting
 396 that the charge changes from -1 to -2 in the pH range: the 2nd step of the
 397 deprotonation. The acid dissociation equilibrium of $K_{\text{a}2}$ is expressed as in Eq. (7) with
 398 its acid dissociation constant (8). The effective electrophoretic mobility is contributed
 399 from both charged species of HA^- and A^{2-} , and it is written as in Eq. (9).



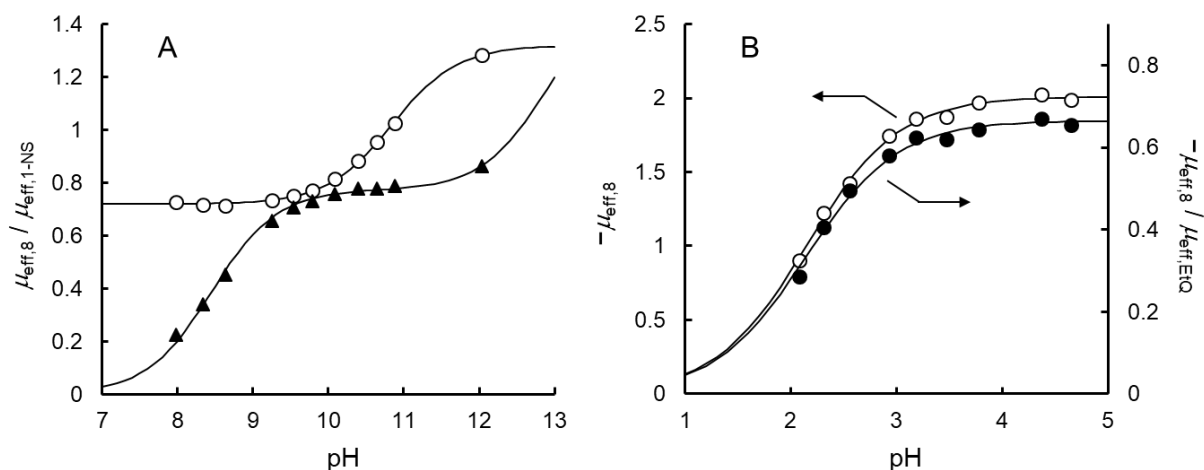
$$401 \quad K_{\text{a}2} = \frac{[\text{H}^+][\text{A}^{2-}]}{[\text{HA}^-]} \quad (8)$$

$$402 \quad \mu_{\text{eff}} = \frac{[\text{HA}^-] \times \mu_{\text{ep,HA}} + [\text{A}^{2-}] \times \mu_{\text{ep,A}}}{[\text{HA}^-] + [\text{A}^{2-}]} = \frac{10^{-\text{pH}} \times \mu_{\text{ep,HA}} + 10^{-\text{p}K_{\text{a}2}} \times \mu_{\text{ep,A}}}{10^{-\text{pH}} + 10^{-\text{p}K_{\text{a}2}}} \quad (9)$$

403

404 Values of $\mu_{ep,HA}$ and $\mu_{ep,A}$ are the electrophoretic mobility of the monoanionic and
405 dianionic species, respectively. A series of the pairs of pH and μ_{eff} were put in Eq. (9),
406 and the values of $\mu_{ep,HA}$, $\mu_{ep,A}$ and pK_{a2} were optimized by a non-linear least-squares
407 analysis in a similar manner after the standardization with 1-NS⁻ as an internal
408 standard. A pK_{a2} value of 10.84 ± 0.02 was obtained by the analysis. Optimized values
409 of standardized $\mu_{ep,HA}$ and $\mu_{ep,A}$ were 0.72 and 1.32, respectively. The standardized
410 $\mu_{ep,A}$ value is 1.83 times to that of $\mu_{ep,HA}$ value, and the twice charge of A²⁻ against HA⁻
411 would be appropriate. The effective electrophoretic mobility of the impurity showed
412 two-steps increase (Figure 4 A), and the increase was also analyzed as two-steps acid
413 dissociation equilibrium, as written in Eq. (6); acid dissociation constants of $pK_{a1} =$
414 8.45 ± 0.02 and $pK_{a2} = 12.91 \pm 0.09$ were determined by the analysis. An LC-MS
415 analysis gave a mass number of 243.09, and the impurity was also LC.

416



417

418 **Figure 4.** Changes in the effective electrophoretic mobility of FL analogue 8. (A) At weakly
419 alkaline conditions. The μ_{eff} values are standardized with $\mu_{eff,1-NS}$. \circ , FL analogue 8; \blacktriangle , impurity.
420 (B) At weakly acidic conditions. \circ , the μ_{eff} values are directly used for the analysis; \bullet , the μ_{eff}
421 values are used for the analysis after standardized with $\mu_{eff,EtQ}$. The curves are drawn with the
422 optimized results. CZE conditions: (A), applied voltage, 25 kV; sample injection, 50 mbar \times 5
423 s; detection wavelength, 220 nm; capillary temperature, 25 $^{\circ}$ C; (B), pressure-assisted CZE
424 under 25 kV applied voltage and 30 mbar pressure assist, other conditions are as in (A).

425

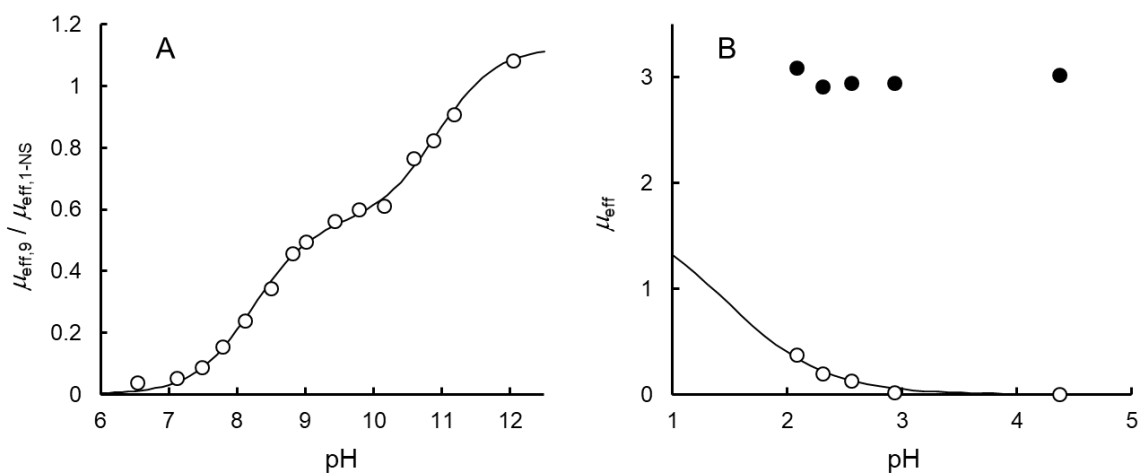
426 3.2.7 Acid dissociation constants of FL analogue 9 at weakly alkaline pH region

427 2-(7,8-Dimethyl-10-isoalloxazolyl)ethyl-L-proline (FL analogue 9) is a triprotic acid, and
428 its charge changes from +1 to -2 by the three-steps acid dissociation reactions of a
429 carboxylic acid moiety, a protonated pyrrolidine moiety, and an imide moiety.

430 Electropherograms are shown in Figure S9, and the changes in μ_{eff} are shown in
431 Figure 5 A after standardized with $\mu_{\text{eff},1\text{-NS}}$. The migration time of FL analogue 9 got
432 longer than the EOF with the increase in pH. Two-steps increase in the μ_{eff} is read out,
433 and the acid dissociation constants of pK_{a2} (protonated pyrrolidine moiety) and pK_{a3}
434 (imide moiety) have been analyzed by Eq. (6) through the μ_{eff} values; $pK_{a2} = 8.23 \pm 0.04$
435 and $pK_{a3} = 10.93 \pm 0.06$ were determined. The pK_a values for the FL analogues
436 determined by the CZE are summarized in Table 2.

437 An acid dissociation constant of FL analogue 9 was also determined by
438 spectrophotometric titration at alkaline pH region. Changes in the absorbance at 356
439 nm was used for the analysis. One step of the absorbance change was observed with
440 a clear isosbestic point at 368 nm, and a pK_a value of 10.74 ± 0.02 was determined.
441 The pK_a value corresponds to the pK_{a3} value at the imide moiety determined by the
442 CZE. However, the spectrum slightly changed in the pH range from 6.7 to 9.4 where
443 the pK_{a2} value was determined by the CZE analysis. The absence of the spectrum
444 shift by the acid dissociation equilibrium would be because of the pyrrolidine moiety
445 being shielded from the resonance skeleton. Therefore, CZE analysis is applicable to
446 such substance without any spectrum shift.

447



448

449 **Figure 5.** Changes in the effective electrophoretic mobility of FL analogue 9. (A) At weakly
450 alkaline conditions. \circ , FL analogue 9 standardized with $\mu_{\text{eff},1\text{-NS}}$. (B) At weakly acidic conditions.
451 \circ , FL analogue 9; \bullet , EtQ⁺. The curves are drawn with the optimized results. CZE conditions:
452 (A), applied voltage, 25 kV; sample injection, 50 mbar \times 5 s; detection wavelength, 220 nm;
453 capillary temperature, 25 °C; (B), pressure-assisted CZE under 25 kV applied voltage and 30
454 mbar pressure assist, other conditions are as in (A).

455

456

457

Table 2. Acid dissociation constants of FL analogues determined in this study

	pK_{a1} ^{a)}	pK_{a2} ^{a)}	pK_{a1} ^{a)}	Remark
Analogue 2	10.21±0.05 10.24±0.04 ^{b)}	N/A ^{c)}	N/A ^{c)}	Degraded at alkaline conditions: hydrolysis of ester moiety.
Analogue 3	10.38±0.04	N/A	N/A	Degraded at storage conditions: LC was formed.
Analogue 4	10.22±0.08	N/A	N/A	Degraded at alkaline conditions: LC was formed.
Analogue 5	10.35±0.04	N/A	N/A	Degraded at storage conditions with light exposure: LC was formed.
Analogue 7	8.07±0.01	(12.96±0.4) ^{d)}	N/A	Impurity of LC was contained.
Analogue 8	2.15±0.02 ^{e)}	10.84±0.02	N/A	
Analogue 9	(1.46±0.03) ^{d),e)}	8.23±0.04 (-) ^{f)}	10.93±0.06 (10.74±0.02) ^{f)}	

458

^{a)} Error: standard error.

459

^{b)} Degraded at alkaline conditions.

460

^{c)} Not applicable.

461

^{d)} Estimated value by extrapolation.

462

^{e)} Determined by pressure-assisted CZE; no standardization of μ_{eff} .

463

^{f)} Determined by spectrophotometric titration.

464

465 3.3 Determination of acid dissociation constants of FL analogues

466 by pressure-assisted CZE

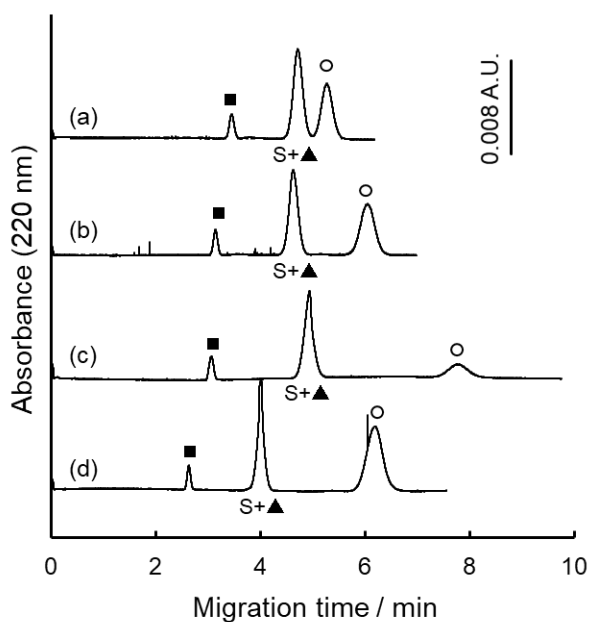
467 Acid dissociation constants of the carboxylic acid moiety on FL analogues 8 and 9
 468 were difficult to analyze by CZE, because their peak signals were not detected at acidic
 469 pH conditions due to the slow EOF. Therefore, pressure-assisted CZE [13,14] was
 470 examined to compensate the slow EOF and to detect the analytes even at the acidic
 471 pH conditions. An assisting air-pressure of 30 mbar was applied to the inlet vial during
 472 the electrophoresis. The migration time of the EOF got faster and the analytes of
 473 interest can be detected by the pressure-assisted CZE.

474 3.3.1 Acid dissociation constant of FL analogue 8 at acidic pH region

475 As noted in the previous section, FL analogue 8 is electrically neutral at acidic pH
 476 conditions and its charge changes from 0 to -1 by the acid dissociation reaction of the
 477 carboxylic acid moiety. Pressure-assisted electropherograms are shown in Figure 6.
 478 FL analogue 8 migrated slower than the EOF, and it is also anionic in this pH range.
 479 The peak widths became wider by applying the pressure compared with the normal

480 CZE, because the analyte in the plug zone is dispersed by the parabolic flow in the
 481 directions of both the tube axis and the tube diameter. However, the effective
 482 electrophoretic mobility of the internal standard, EtQ⁺, was affected little by the
 483 pressure, and therefore, the effective electrophoretic mobility of the analyte would be
 484 measured properly, and it would be used for the pK_a analysis. Changes in μ_{eff} of FL
 485 analogue 8 are shown in Figure 4 B; both directly measured μ_{eff} values and
 486 standardized μ_{eff} values with EtQ⁺ were used for the analysis. Since anionic internal
 487 standard of 1-NS⁻ was not detected even by the pressure-assisted CE, cationic EtQ⁺
 488 was used for the standardization. Fortunately, protonated species of FL analogue 8 is
 489 electrically neutral, its electrophoretic mobility is zero and Eq. (3) was used for the
 490 analysis on the basis of an acid dissociation equilibrium (1). A pK_{a1} value of 2.15±0.02
 491 was obtained with the direct analysis of μ_{eff} values, whereas a pK_{a1} value of 2.14±0.03
 492 was obtained after the standardization with EtQ⁺. Therefore, the standardization
 493 worked well.

494



495

496 **Figure 6.** Electropherograms of FL analogue 8
 497 at acidic pH conditions by the pressure-
 498 assisted CZE. pH conditions: (a), 2.08; (b),
 499 2.56; (c), 3.47; (d), 4.65. Symbols: o, FL
 500 analogue 8; ▲, LC as a degradant; ■, EtQ⁺; S,
 501 solvent (EOF). Sample solution: 6×10^{-5} mol L⁻¹
 502 FL analogue 8 + 3×10^{-5} mol L⁻¹ EtQ⁺ (I.S.) +
 503 3 % (v/v) ethanol. Separation buffers are written
 504 in the text. CZE conditions: applied voltage, 25
 505 kV; assist pressure, 30 mbar; sample injection,

506 50 mbar × 5 s; detection wavelength, 220 nm;
507 capillary temperature, 25 °C.

508

509 **3.3.2 Acid dissociation constants of FL analogue 9 at acidic pH region**

510 An acid dissociation constant of FL analogue 9 was also examined by the pressure-
511 assisted CZE. Its charge changes from +1 to 0 by the acid dissociation reaction of the
512 carboxylic acid moiety, and the dissociated species is zwitterion. Electropherograms
513 are shown in Figure 7; broad peaks are also detected as in the case of FL analogue
514 8. It can be seen from Figure 7 that FL analogue 9 migrated faster than the EOF at
515 acidic pH conditions and it is cationic. Although only a broad peak is detected the EOF
516 position at pH 2.56 (b), the broad peak was found to be composed of two overlapped
517 peaks of FL analogue 9 and the EOF when detected at 254 nm. Changes in the
518 electrophoretic mobility are shown in Figure 5 B. FL analogue 9 becomes more
519 cationic at acidic conditions. Different from FL analogue 8, the electrophoretic mobility
520 of the protonated species of H₃A⁺ is not zero, and the value is difficult to measure. The
521 acid dissociation equilibrium and its acid dissociation constant are written as in Eq.
522 (10) and (11), respectively. The effective electrophoretic mobility is contributed from
523 the positively charged species, H₃A⁺, and it is given in Eq. (12).

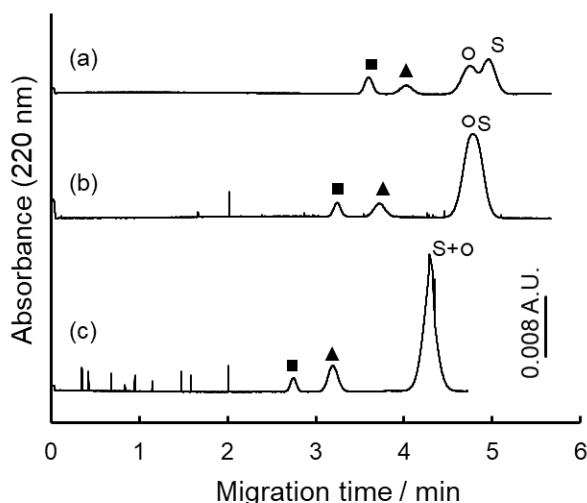


$$525 K_a = \frac{[\text{H}^+][\text{H}_2\text{A}]}{[\text{H}_3\text{A}^+]} \quad (11)$$

$$526 \mu_{\text{eff}} = \frac{[\text{H}_3\text{A}^+] \times \mu_{\text{ep,H3A}}}{[\text{H}_3\text{A}^+] + [\text{H}_2\text{A}]} = \frac{10^{-\text{pH}} \times \mu_{\text{ep,H3A}}}{10^{-\text{pH}} + 10^{-\text{p}K_a}} \quad (12)$$

527 Value of $\mu_{\text{ep,H3A}}$ is the electrophoretic mobility of the monocationic species. Another
528 problem is that CZE measurements at pH conditions below 2 is also difficult owing to
529 the high salt concentrations and the generated Joule's heat. To estimate the acid
530 dissociation constant of the carboxylic acid moiety of FL analogue 9, the
531 electrophoretic mobility of the cationic species of +1 charged one was assumed to be
532 equal to that of the anionic species of -1 charged one. An acid dissociation constant
533 of 1.46 ± 0.03 was estimated under such assumption.

534



535

536 **Figure 7.** Electropherograms of FL analogue 9
 537 at acidic pH conditions by pressure-assisted
 538 CZE. pH conditions: (a), 2.08; (b), 2.56; (c),
 539 4.37. Symbols: ○, FL analogue 9; ▲, impurity;
 540 ■, EtQ⁺; S, solvent (EOF). Sample solution:
 541 $6 \times 10^{-5} \text{ mol L}^{-1}$ FL analogue 9 + $3 \times 10^{-5} \text{ mol L}^{-1}$
 542 EtQ⁺ (I.S.) + 3 % (v/v) ethanol. Separation
 543 buffers are written in the text. CZE conditions:
 544 applied voltage, 25 kV; assist pressure, 30
 545 mbar; sample injection, 50 mbar × 5 s;
 546 detection wavelength, 220 nm; capillary
 547 temperature, 25 °C.

548 **4 Concluding remarks**

549 In this study, acid dissociation constants were determined by CZE for a series of
 550 molecular catalyst candidates of FL analogues. Changes in the μ_{eff} by the protonation
 551 or deprotonation were used for the CZE analysis. The CZE analysis was proved to be
 552 useful for the separation of the target analyte from the coexisting substances including
 553 degraded species and impurities. The CZE analysis is also applicable to such
 554 substances as without spectrum shift. Pressure-assisted CZE was also utilized for the
 555 measurements of the effective electrophoretic mobility at weakly acidic pH conditions,
 556 where the electroosmotic flow is slow.

557 **Acknowledgements**

558 This work was supported by a Grant-in-Aid for Scientific Research (C) (No. 17K05903)
 559 from the Japan Society for the Promotion of Sciences (JSPS). The authors
 560 acknowledge to Dr. Shoko Ueta (Tokushima University) for the LC-MS measurements.

561 **Conflict of interest**

562 The authors have declared no conflict of interest.

563 **5 References**

564 [1] Iida, H., Imada, Y., Murahashi, S.-I., *Org. Biomol. Chem.* 2015, 13, 7599-7613.

565 [2] Tagami, T., Arakawa, Y., Minagawa, K., Imada, Y., *Org. Lett.* 2019, 21, 6978-6982.

566 [3] Imada, Y., Kitagawa, T., Ohno, T., Iida, H., Naota, T., *Org. Lett.* 2010, 12, 32-35.

567 [4] Arakawa, Y., Yamanomoto, K., Kita, H., Minagawa, K., Tanaka, M., Haraguchi, N.,
568 Itsuno, S., Imada, Y., *Chem. Sci.* 2017, 8, 5468-5475.

569 [5] Sheraz, M. A., Kazi, S. H., Ahmed, S., Anwar, Z., Ahmad, I., *Beilstein J. Org. Chem.*
570 2014, 10, 1999-2012.

571 [6] Stanojević, J. S., Zvezdanović, J. B., Marković, D. Z., *Monatsh. Chem.* 2015, 146,
572 1787-1794.

573 [7] Andradi, M., Buglyo, P., Zekany, L., Gaspar, A., *J. Pharm. Biomed. Anal.* 2007, 44,
574 1040-1047.

575 [8] Takayanagi, T., Motomizu, S., *Chem. Lett.* 2001, 30, 14-15.

576 [9] Örnkvist, E., Linusson, A., Folestad, S., *J. Pharm. Biomed. Anal.* 2003, 33, 379-
577 391.

578 [10] Takayanagi, T., Tabara, A., Kaneta, T., *Anal. Sci.* 2013, 29, 547-552.

579 [11] Takayanagi, T., Itoh, D., Mizuguchi, H., *Chromatography* 2016, 37, 105-109.

580 [12] Imada, Y., Iida, H., Ono, S., Masui, Y., Murahashi, S.-I., *Chem. Asian J.* 2006, 1,
581 136-147.

582 [13] Wang, J. L., Xu, X. J., Chen, D. Y., *J. Pharm. Biomed. Anal.* 2014, 88, 22-26.

583 [14] Konášová, R., Dyrtrtová, J. J., Kašička, V., *J. Chromatogr. A* 2015, 1408, 243-249.

584 [15] The R Project for Statistical Computing, <https://www.r-project.org/>.

585 [16] Hirabayashi, K., Hanaoka, K., Takayanagi, T., Toki, Y., Egawa, T., Kamiya, M.,
586 Komatsu, T., Ueno, T., Terai, T., Yoshida, K., Uchiyama, M., Nagano, T., Urano, Y.,
587 *Anal. Chem.* 2015, 87, 9061-9069.

588 [17] O'Neil, M. J. (Ed.), *The Merck Index 14th Ed.*, Merck Research Laboratories,
589 Whitehouse Station, NJ 2006, p. 1413.

590 [18] Prukala, D., Sikorska, E., Koput, J., Khmelinskii, I., Karolczak, J., Gierszewski, M.,
591 Sikorski, M., J. Phys. Chem. A 2012, 116, 7474-7490.

592 [19] Ghasemi, J., Ghobadi, S., Abbasi, B., Kubista, M., J. Kor. Chem. Soc. 2005, 49,
593 269-277.

594

595 **Supporting information**

596 **Supporting information file:** Syntheses of FL analogues 2, 3, 4, 5, 7, 8, and 9 are
597 described. Typical electropherograms and the changes in the effective mobility are
598 shown in Figures S1, S2, S4, S5, S6, and S7 for FL analogues 1, 2, 3, 4, 5, and 7,
599 respectively. Typical electropherograms are shown in Figures S8 and S9 for FL
600 analogues 8 and 9, respectively. LC-MS chromatograms for alkaline-treated FL
601 analogues 2 are shown in Figure S3.

602